Green Chemistry

PAPER

View Article Online
View Journal | View Issue



Cite this: *Green Chem.*, 2025, **27**, 3477

# Engineering budding yeast for the *de novo* synthesis of valuable flavanone derivatives†

Si-Yu Zhu,[a,b] Na Li,[a,b] Zhi-Hua Liu,*[a,b] Ying-Jin Yuan [a,b] and Bing-Zhi Li *[a,b]

Received 18th October 2024,
Accepted 17th January 2025

DOI: 10.1039/d4gc05241b

rsc.li/greenchem

Flavonoids, such as homoeriodictyol derivatives, hold significant value in nutraceuticals, foods, and pharmaceuticals. Microbial synthesis of these products has emerged as a powerful approach due to its sustainability and environmental friendliness. However, constructing microbial cell factories of homoeriodictyol derivatives is often challenged by the lack of a biosynthesis pathway and the poor performance of endogenous metabolic networks. Here, an efficient *Saccharomyces cerevisiae* cell factory was designed and metabolically engineered for the *de novo* biosynthesis of homoeriodictyol 7-*O*-glucoside. Relieving the feedback inhibition and overexpressing the key enzymes successfully achieved the biosynthesis of homoeriodictyol with a titer of 174.0 mg $L^{-1}$. Enzyme screening strategies explored missing glycosyltransferases and unveiled the homoeriodictyol 7-*O*-glucoside synthesis pathway for the first time. Blocking the glycoside hydrolysis pathway improved the titer of homoeriodictyol 7-*O*-glucoside by a substantial 7.2-fold. Metabolically regulating NADPH regeneration reduced the intermediate accumulation by 91.3%, while strengthening uridine diphosphate-glucose and substrate supply further boosted the homoeriodictyol 7-*O*-glucoside production. Altogether, these advancements led to a record homoeriodictyol 7-*O*-glucoside titer of 600.2 mg $L^{-1}$ and a yield of 12.2 mg $g^{-1}$ glucose. Overall, the versatile *S. cerevisiae* cell factory shows the potential to synthesize homoeriodictyol 7-*O*-glucoside, contributing to the green and sustainable production of natural products.



**Green foundation**

1. This work aims to design a *Saccharomyces cerevisiae* cell factory for the synthesis of a complex flavonoid glycoside, homoeriodictyol 7-*O*-glucoside. Microbial cell factories using biocatalysts can streamline the structural modification of compounds, enabling a more efficient and green synthesis mode. Microbial conversion processes utilize renewable, biodegradable feedstocks for natural products, which lowers the overall carbon footprint, contributing to a sustainable circular bioeconomy.
2. This work demonstrated the feasibility of utilizing microbial systems to perform environmentally benign transformations with high selectivity and yield, presenting an effective and sustainable alternative to traditional synthetic routes. The versatile strategies of metabolic engineering and fermentation optimization achieved a record homoeriodictyol 7-*O*-glucoside titer of 600.2 mg $L^{-1}$.
3. Future work will focus on enhancing the synthesis efficiency of homoeriodictyol 7-*O*-glucoside by exploring advanced biocatalysis techniques, utilizing renewable feedstocks, and developing green separation strategies for sustainable large-scale production.

## 1. Introduction

Natural products are small bioactive molecules naturally derived from living organisms, such as plants, animals, fungi, and microorganisms.[1] Flavonoids, valuable natural phenolic compounds known for their anti-inflammatory, antiviral, and anti-cancer properties, are widely used in nutraceutical and pharmaceutical supplements.[2–4] Some flavonoids and their derivatives, such as homoeriodictyol and homoeriodictyol glu-

[a]*Frontiers Science Center for Synthetic Biology and Key Laboratory of Systems Bioengineering (Ministry of Education), School of Chemical Engineering and Technology, Tianjin University, Tianjin 300072, China. E-mail: bzli@tju.edu.cn*
[b]*Frontiers Research Institute for Synthetic Biology, Tianjin University, Tianjin 301799, China. E-mail: zhliu@tju.edu.cn*

†Electronic supplementary information (ESI) available. See DOI: https://doi.org/10.1039/d4gc05241b

coside, can also serve as taste modifiers in the food industry due to their remarkable bitter-masking ability.[5–7] *O*-Glycosylation greatly improves the biological activity of flavonoids, such as anti-HIV activity, tyrosinase inhibition, and antistress activity.[8] Glycosylation also relieves the toxicity of flavonoid aglycones to cells and improves the bioavailability.[9,10] Homoeriodictyol 7-*O*-glucoside is the glycosylated product at the 7-OH position of homoeriodictyol, exhibiting anti-angina effects and superior bitter-masking capabilities, alongside the intrinsic biological activity of flavanones.[11,12]

Homoeriodictyol 7-*O*-glucoside has traditionally been obtained through chemical synthesis and plant extraction. Advanced chemical synthesis is scalable and capable of producing target products with high purity.[14] However, the chemical synthesis of homoeriodictyol 7-*O*-glucoside requires expensive precursors, such as phloroglucinol, and depends on high temperatures, pressures, and other resource-intensive conditions.[11] Additionally, chemical synthesis of structurally complex natural products can be challenging and often inefficient.[15] Plant extraction is a mild process for obtaining natural products, requiring minimal infrastructure compared to microbial or chemical synthesis. However, it typically involves the use of large volumes of organic solvents, such as methanol and chloroform, to isolate homoeriodictyol 7-*O*-glucoside.[16,17] It has been reported that 98 mg of homoeriodictyol 7-*O*-glucoside was extracted from 10 kg of *Viscum album* L. using 2.75 kg of methanol and multiple partitioning steps with *n*-hexane, chloroform, and *n*-butanol.[16] Besides, the low extraction yields require larger areas of land to cultivate *Viscum album* L., posing challenges to maintaining a sustainable supply.

Microbial cell factories offer a powerful and green platform for synthesizing complex bioactive natural products from renewable resources.[18–20] For example, homoeriodictyol, the key precursor of homoeriodictyol 7-*O*-glucoside, has been biosynthesized in microbial cell factories. Homoeriodictyol biosynthesis typically begins with two aromatic monomers, ferulic acid and *p*-coumaric acid. The biosynthesis pathways of homoeriodictyol from ferulic acid were first elucidated in *Escherichia coli*, involving key enzymes such as 4-coumarate-CoA ligase (4CL), chalcone synthase (CHS), and chalcone isomerase (CHI).[21–23] Recently, based on the structure analysis and multiple sequence alignment, redesigning the rate-limiting enzyme CHS had increased the homoeriodictyol titer to 0.33 mM.[24] Additionally, the biosynthesis pathway of homoeriodictyol was also constructed in *Streptomyces albidoflavus* by expressing tyrosine ammonia lyase (TAL), 4CL, CHS, CHI, flavonoid 3′-monooxygenase (F3′H), cytochrome P450 reductase, and 3′-*O*-methyltransferase. A transcriptomics study of *S. albidoflavus* revealed the tyrosine catabolism pathway, indicating the potential role of 4-hydroxyphenylpyruvate dioxygenase in tyrosine catabolism. Inactivating the 4-hydroxyphenylpyruvate dioxygenase coding gene facilitated tyrosine accumulation, thereby achieving a homoeriodictyol titer of 1.34 mg $L^{-1}$.[25] However, substrate–enzyme incompatibility and poor heterologous expression of key enzymes still hinder homoeriodictyol production in *E. coli* and *Streptomyces*. Moreover, the limited membrane structures of bacteria impede the efficient exploration of homoeriodictyol biosynthesis through the *p*-coumaric acid branch, which involves cytochrome reductase-mediated reactions.

Alternatively, *Saccharomyces cerevisiae*, a model organism, offers abundant membrane structures conducive to the expression of cytochrome reductases. Consequently, the homoeriodictyol biosynthesis from *p*-coumaric acid in *S. cerevisiae* has emerged as a promising pathway.[26] This newly proposed pathway includes the key enzymes 4CL from *Petroselinum crispum*, CHS from *Petunia* × *hybrida*, CHI from *Medicago sativa*, F3′H from *Arabidopsis thaliana*, cytochrome P450 reductase 1 (ATR1) from *A. thaliana*, and flavone 3′-*O*-methyltransferase (ROMT-9) from *Oryza sativa subsp. Japonica*. Combinatorial strategies of metabolic engineering and enzyme engineering yielded a homoeriodictyol titer of 3.2 mM from *p*-coumaric acid in *S. cerevisiae*.

*De novo* biosynthesis from renewable glucose is an encouraging process, since it reduces reliance on expensive raw materials, simplifies production processes, and potentially promotes the feasibility of natural product manufacturing.[13,27,28] However, the *de novo* biosynthesis pathway of homoeriodictyol 7-*O*-glucoside remains unclear due to the lack of the functional key enzymes. Additionally, the hydrolysis of flavonoid glycosides by chassis microorganisms hampers the effective production of homoeriodictyol 7-*O*-glucoside. The imbalance between the redox power required for cell growth and biosynthesis, along with the limited availability of glycosyl donors, also restricts the synthesis of homoeriodictyol 7-*O*-glucoside. Therefore, tapping into the *de novo* biosynthesis pathway and harnessing metabolic engineering strategies could accelerate the efficient production of homoeriodictyol 7-*O*-glucoside.

This work aims to design a *S. cerevisiae* cell factory capable of synthesizing homoeriodictyol 7-*O*-glucoside. Efforts had been made to establish the *de novo* synthesis pathway of homoeriodictyol from renewable glucose. Both endogenous and heterologous pathways were modulated to enhance the supply of homoeriodictyol. Missing glycosyltransferases were explored to convert homoeriodictyol into homoeriodictyol 7-*O*-glucoside. Subsequently, metabolic engineering strategies were implemented to create a suitable platform strain for glucoside synthesis and guarantee more reducing power and glycosyl donors for the homoeriodictyol 7-*O*-glucoside synthesis. These strategies could contribute to the green and sustainable synthesis of complex bioactive natural products.

## 2. Materials and methods

### 2.1. Chemical and reagents

Glucose, NaCl and amino acid powder were purchased from Shanghai Sangon Biotech Co., Ltd. Tryptone, yeast extract, and yeast nitrogen base without amino acids were purchased from Thermo Fisher Scientific. Ethanol, acetic acid, methanol and acetonitrile were purchased from Shanghai Aladdin Reagents

 

Co., Ltd. The flavonoid standards were all purchased from Shanghai Yuanye Biotech Co., Ltd. Trans1-T1 competent cells were purchased from Beijing TransGen Biotech Co., Ltd. KOD FX DNA polymerase was purchased from Shanghai TOYOBO Biotech Co., Ltd. BM seamless cloning kits were purchased from Beijing Biomed Gene Technology Co., Ltd. 2 × Rapid Taq Master Mix was purchased from Nanjing Vazyme Biotech Co., Ltd. DNA gel purification kits and plasmid extraction kits were purchased from Beijing TIANGEN Biotech Co., Ltd.

### 2.2. Strains and media

*S. cerevisiae* CEN.PK2-1D (MATα; ura3-52; trp1-289; leu2-3, 112; his3Δ1; MAL2-8C; SUC2) was used as the host strain in the present study. The plasmids were constructed and amplified in *E. coli Trans*1-T1 competent cells. *S. cerevisiae* strains without plasmids were cultured in yeast extract-peptone-dextrose (YPD) medium consisting of 20 g $L^{-1}$ tryptone, 20 g $L^{-1}$ glucose, and 10 g $L^{-1}$ extract.[29] *S. cerevisiae* strains with plasmids were cultured in synthetic complete drop-out (SC) medium consisting of 20 g $L^{-1}$ glucose, 6.7 g $L^{-1}$ yeast nitrogen base without amino acids, and 2 g $L^{-1}$ amino acid mixture lacking specific amino acids.[30] All *S. cerevisiae* strains were cultivated at 30 °C. *E. coli* strains were incubated in Luria–Bertani medium consisting of 10 g $L^{-1}$ tryptone, 10 g $L^{-1}$ NaCl, and 5 g $L^{-1}$ yeast extract, supplemented with 50 μg $mL^{-1}$ kanamycin or 100 μg $mL^{-1}$ ampicillin when needed. All *E. coli* strains were cultivated at 37 °C.[31]

### 2.3. Genetic manipulation

The engineered strains and constructed plasmids are listed individually in Tables S1 and S2.† The heterologous genes and primers were synthesized by Tsingke Biotechnology Inc. (Beijing, China). The endogenous genes were amplified from the genomic DNA of *S. cerevisiae* CEN. PK2-1D. The *aroL* gene, encoding shikimate kinase 2, was obtained from *E. coli* (Accession Number: P0A6E1). The *PDH1* gene, encoding prephenate dehydrogenase, was obtained from *Medicago truncatula* (Accession Number: G7J2E9). The *ACS* gene, encoding acetyl-coenzyme A synthetase, was obtained from *Salmonella enterica* (Accession Number: Q8ZKF6). The *PAL2* gene, encoding phenylalanine ammonia-lyase 2, was obtained from *Arabidopsis thaliana* (Accession Number: P45724). The *C4H* gene, encoding *trans*-cinnamate 4-monooxygenase, was obtained from *A. thaliana* (Accession Number: P92994). The *ATR2* gene, encoding cytochrome P450 reductase 2, was obtained from *A. thaliana* (Accession Number: Q9SUM3). The *TAL* gene, encoding tyrosine ammonia-lyase, was obtained from *Flavobacterium johnsoniae* (Accession Number: A5FKY3). The *GT2* genes, encoding UDP-glycosyltransferases, were obtained from Tobacco and *A. thaliana* (Accession Number: Q8RU71 and Q8VZE9). The *UGT73C6* and *UGT73B2* genes, encoding UDP-glycosyltransferases, were obtained from *A. thaliana* (Accession Number: Q9ZQ95 and Q94C57). The *GT4* gene, encoding UDP-glycosyltransferase, was obtained from *Dianthus chinensis* L. (Accession Number: Q60FE9). The *VHb* gene, encoding bacterial hemoglobin, was obtained from *Vitreoscilla stercoraria* (Accession Number: P04252).

The construction of expression cassettes and site-directed mutagenesis were according to the previous work in the lab.[26] The chromosomal integration of the pathway genes and deletion of the undesired genes were achieved using the CRISPR/Cas9 system and yeast homologous recombination.[32] The CRISPR plasmid contains the Cas9 and sgRNA expression cassettes. The gRNA is usually the 20 bp fragment upstream of the PAM sequence (NGG) of the target genomic site.[33] For the integration of DNA fragments, yeast transformation using the lithium acetate/single-stranded carrier (LiAc/SS) method was applied to introduce the CRISPR plasmid, linker fragments and inserted DNA fragments to the host strain.[30] The linker fragment contains the homologous arms of the target genomic integration sites and the homologous arms of the inserted pathway gene expression cassette. Adjacent inserted DNA fragments possess about 400 bp homologous arms, and the terminator of the previous expression cassette is usually added to the front of the promoter of the next expression cassette. As for the deletion of undesired genes, only the CRISPR plasmid and the linker fragment were transformed into the host strain, and the linker fragment contains the upstream homologous arm and downstream homologous arm of the deleted gene.

### 2.4. Fermentation strategies

For batch-fermentation, the engineered strains were first cultivated in 5 mL of SC medium without uracil at 30 °C, 220 rpm for 12 h to obtain seed culture. The seed culture was then inoculated into 30 mL of YPD medium with an initial $OD_{600}$ of 0.1, and the initial glucose concentration was adjusted to 30 g $L^{-1}$ or 40 g $L^{-1}$ optionally. For fed-batch fermentation, the seed culture was inoculated into 30 mL of YPD medium with an initial $OD_{600}$ of 0.1 and was fed with 500 g $L^{-1}$ concentrated glucose solution at 24 h or 24 h and 48 h to ensure that the glucose concentration in the fermentation was 10 g $L^{-1}$ at these time points. For high-density fermentation, the seed culture was inoculated into 50 mL of SC medium without uracil. After 12 h cultivation, the culture was centrifuged at 1500 g for 5 min, and the supernatant was discarded. The concentrated cells were used to inoculate into the 30 mL of YPD medium with the glucose concentration of 40 g $L^{-1}$. The initial $OD_{600}$ was set to 20, 30, or 40. The fermentation was conducted at 30 °C, 220 rpm for 72 h or 96 h.

### 2.5. Quantification methods

As for the quantification of aromatic compounds in the fermentation broth, the fermentation samples were analyzed by high-performance liquid chromatography (HPLC). 300 μL of ethanol was added to 300 μL of the fermentation broth and mixed by vortex oscillation. The mixture was centrifuged at 12 000 rpm for 2 min. The supernatant was filtered using a 0.22 μm organic filter, and then the concentrations of the aromatic compounds were determined on a Waters e2695 HPLC instrument (Waters Corp., Milford, MA, USA) connected to a photodiode array detector. A C18 column (25 cm × 4.6 mm,

5 μm) (Thermo Scientific, Wilmington, DE, USA) was used to separate the products and the quantification was conducted at 290 nm. The detection program was described comprehensively in the previous study.[26] The fermentation results represent the mean value of two separate biological replicates ($n$ = 2), and error bars show the standard deviation. Significance ($p$-value) was accessed by a one-tailed, two-sample unequal variance $t$-test (*$p$ < 0.1, **$p$ < 0.05, ***$p$ < 0.01).

## 3. Results and discussion

### 3.1. Constructing the *de novo* biosynthesis pathway of homoeriodictyol

The *de novo* biosynthesis of homoeriodictyol 7-*O*-glucoside from glucose involves multiple reactions catalyzed by heterologous enzymes in *S. cerevisiae*. Efficient biosynthesis of homoeriodictyol is essential for the subsequent synthesis of homoeriodictyol 7-*O*-glucoside. However, the supply of homoeriodictyol is limited by the unavailability of functional pathways and the poor expression of heterologous enzymes. Moreover, the inherent metabolic fluxes in *S. cerevisiae* impose additional constraints on the *de novo* biosynthesis of homoeriodictyol. The biosynthesis route of homoeriodictyol from *p*-coumaric acid was elaborated previously.[26] Therefore, developing a pathway from glucose to *p*-coumaric acid based on the existing biosynthesis route, while alleviating bottlenecks in the metabolic regulation, would enhance the supply of homoeriodictyol (Fig. 1a).

Tyrosine and phenylalanine, originating from the aromatic amino acid biosynthesis pathway, serve as the primary building blocks for various aromatic natural products. The biosynthesis pathway of *p*-coumaric acid from tyrosine was first constructed in the eriodictyol-producing strain Yeri001.[26] *Fj*TAL was identified as a specific enzyme capable of converting tyrosine into *p*-coumaric acid.[34] Hence, the constitutive expression of *Fj*TAL was conducted under the control of the strong promoter $P_{TEF1}$, and the resulting expression cassette of *FjTAL* was integrated into the chromosomal locus *PDC5* of Yeri001, obtaining strain YTAL001. Stable expression of *Fj*TAL in YTAL001 resulted in an eriodictyol titer of 15.2 mg $L^{-1}$ from glucose, demonstrating *Fj*TAL's effectiveness in channeling carbon flux toward eriodictyol synthesis (Fig. 1b).

The biosynthesis pathway of *p*-coumaric acid from phenylalanine was subsequently explored in YTAL001. *At*PAL2 efficiently converts phenylalanine into cinnamic acid, while *At*C4H and ATR2 further catalyze the conversion of cinnamic acid to *p*-coumaric acid. Additionally, the endogenous enzyme CYB5 in *S. cerevisiae* expedites the catalytic performance of cytochrome *At*C4H.[35,36] To ensure effective expression of these enzymes, *At*PAL2, *At*C4H, ATR2, and CYB5 were expressed using the strong promoters of $P_{TEF1}$, $P_{GPM1}$, $P_{TPI1}$, and $P_{TDH3}$, respectively. Strain YTP001 was obtained by inserting the expression cassettes into the chromosomal loci between *TKL2* and *TEF2* in YTAL001. Introducing the *p*-coumaric acid synthesis pathway from phenylalanine resulted in a significant increase in eriodictyol titer, reaching 109.9 mg $L^{-1}$. Notably, the efficiency of the phenylalanine branch was markedly higher than that of the tyrosine branch, owing to the superior catalytic abilities of *At*PAL2, *At*C4H, ATR2, and CYB5 (Fig. 1b).

Feedback inhibition and insufficient expression of key enzymes in the shikimate pathway are major rate-limiting factors that impede the biosynthesis of natural aromatic products. To further increase eriodictyol titer, it is crucial to address these bottlenecks in the shikimate pathway. 3-Deoxy-D-arabinoheptulosonate 7-phosphate (DAHP) synthase (ARO4) catalyzes the condensation of phosphoenolpyruvate (PEP) and erythrose 4-phosphate (E4P) to form DAHP, while chorismate mutase (ARO7) converts chorismic acid to prephenate. Both ARO4 and ARO7 are allosterically inhibited by tyrosine.[37] To overcome this inhibition, feedback-insensitive variants $ARO4^{K229L}$ and $ARO7^{G141S}$ were introduced into YTP001, leading to a significant 20% increase in eriodictyol titer (Fig. 1c). Shikimate kinase is the rate-limiting enzyme in the tyrosine and phenylalanine biosynthesis pathway. Introducing heterologous shikimate kinase *Ec*aroL is an effective strategy to channel more flux toward *p*-coumaric acid.[38,39] Additionally, overexpressing prephenate dehydrogenase (PDH1) can improve the availability of tyrosine, further boosting the synthesis of *p*-coumaric acid.[39] By overexpressing *Ec*aroL and *Mt*PDH1 in YTP002, the eriodictyol titer of YTP004 increased to 209.2 mg $L^{-1}$, representing a 60.0% improvement (Fig. 1c). These results indicated that engineering the shikimate pathway facilitated the eriodictyol biosynthesis.

To further improve the eriodictyol titer, fine-tuning the malonyl-CoA supply was implemented as a strategic approach. Flavonoid biosynthesis is typically constrained by the limited accessibility of malonyl-CoA in the cytosol, which is crucial for the conversion of *p*-coumaroyl-CoA to naringenin chalcone catalyzed by CHS.[40] Modulating the pyruvate dehydrogenase (PDH) bypass holds the promise to boost the malonyl-CoA supply in the cytosol. The variants $Se\text{ACS}^{L641P}$ and $ACC1^{S659A/S1157A}$ have shown enhanced catalytic activity compared to the native enzymes in *S. cerevisiae*.[41,42] To evaluate their performance, $Se\text{ACS}^{L641P}$ and $ACC1^{S659A/S1157A}$ were introduced into YTP004 sequentially. However, the resulting strains did not show a significant improvement in eriodictyol synthesis performance (Fig. 1c). The results indicated that the malonyl-CoA supply was not yet a limiting factor. ROMT-9 from *O. sativa* has been reported to catalyze the conversion of eriodictyol to homoeriodictyol.[43] To obtain the homoeriodictyol-producing strain, the expression cassette of the variant $ROMT\text{-}9^{N135T/I324M}$ was integrated into the chromosomal locus *ARO10* of YTP004.[26] *S*-Adenosyl-L-methionine (SAM) is the methyl donor for methylation, and low availability of SAM in *S. cerevisiae* commonly restricts the efficient biosynthesis of methylated products.[26] A SAM regeneration system was thus introduced to strengthen the methylation of eriodictyol. SAM provides eriodictyol with a methyl group and then turns into *S*-adenosyl-L-homocysteine (SAH), the synthesis precursor of SAM. SAH hydrolase (SAH1) in *S. cerevisiae* is responsible for converting SAH to L-homocysteine and adenosine; however,

 

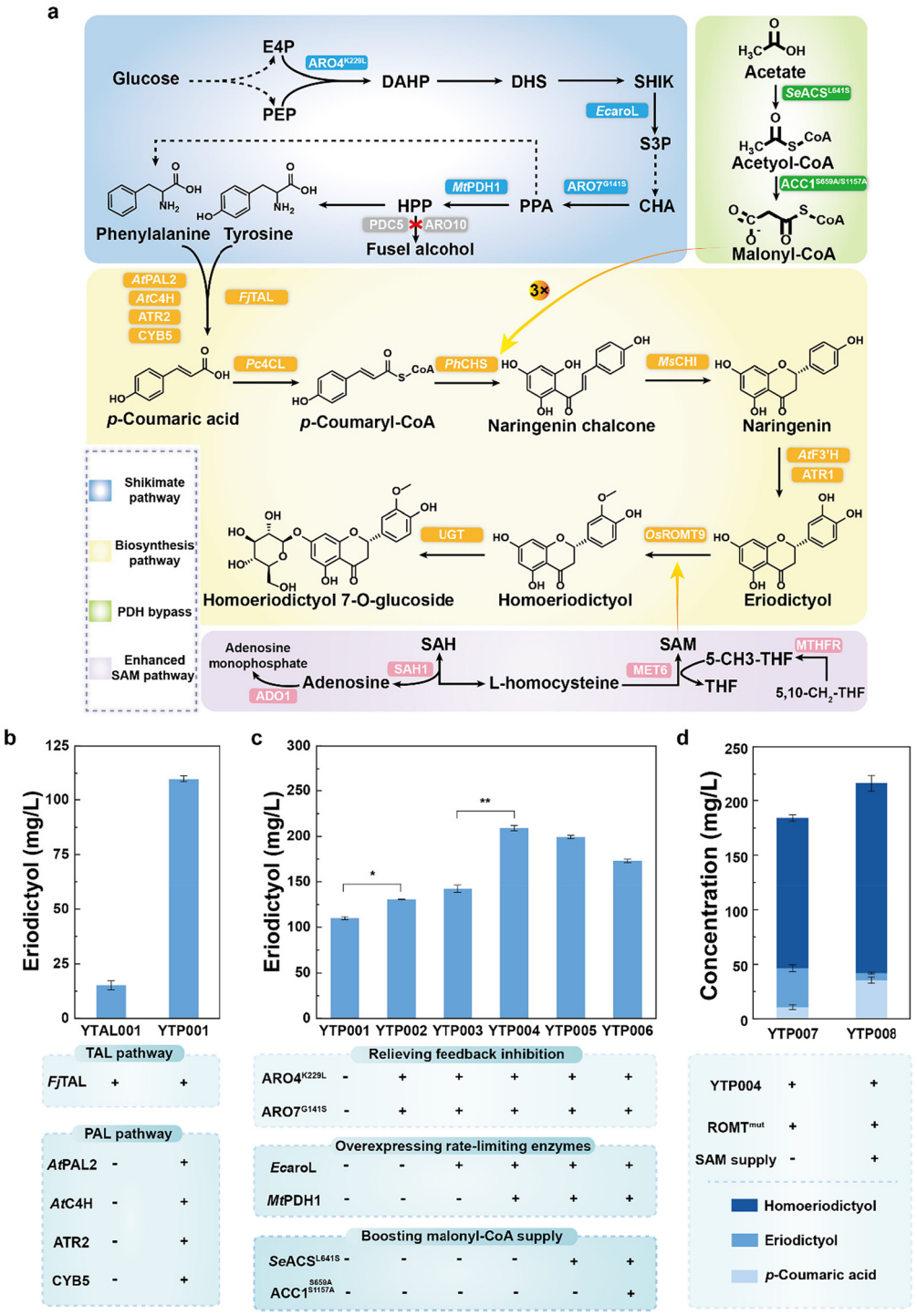


**Fig. 1** The construction of the *de novo* biosynthesis pathway of homoeriodictyol in *S. cerevisiae*. (a) The *de novo* biosynthesis pathway of homoeriodictyol 7-*O*-glucoside. (b) The effect of the phenylalanine branch on eriodictyol production. (c) The effect of relieving the feedback inhibition, overexpressing rate-limiting enzymes, and boosting malonyl-CoA supply on eriodictyol production. (d) Integration of the enhanced *O*-methylation pathway achieved efficient homoeriodictyol production. *ARO4*$^{K229L}$: feedback-insensitive variant of DAHP synthase; *EcaroL*: shikimate kinase; *ARO7*$^{G141S}$: feedback-insensitive variant of chorismate mutase; *MtPDH1*: prephenate dehydrogenase; *SeACS*$^{L641S}$: acetyl-CoA synthetase; *ACC1*$^{S659A/S1157A}$: acetyl-CoA carboxylase; *AtPAL2*: phenylalanine ammonia-lyase 2; *AtC4H*: *trans*-cinnamate 4-monooxygenase; *ATR2*: cytochrome P450 reductase 2; *CYB5*: cytochrome b5; *FjTAL*: tyrosine ammonia-lyase; *Pc4CL*: 4-coumarate-CoA ligase; *PhCHS*: chalcone synthase; *MsCHI*: chalcone isomerase; *AtF3'H*: flavonoid 3'-monooxygenase; *ATR1*: cytochrome P450 reductase 1; *OsROMT-9*: 3'-*O*-methyltransferase; *UGT*: UDP-glycosyltransferase; *ADO1*: adenosine kinase; *SAH1*: SAH hydrolase; *MET6*: homocysteine *S*-methyltransferase; *MTHFR*: methylenetetrahydrofolate reductase. E4P: erythrose-4-phosphate; PEP: phosphoenolpyruvate; DAHP: 3-deoxy-D-arabino-heptulosonate-7-phosphate; DHS: 3-dehydro-shikimate; SHIK: shikimate; CHA: chorismic acid; PPA: prephenate; HPP: *para*-hydroxy-phenylpyruvate; SAH: *S*-adenosyl L-homocysteine; SAM: *S*-adenosyl-L-methionine; 5-$CH_3$-THF: 5-methyl-tetrahydrofolic acid; THF: tetrahydrofolate; 5,10-$CH_2$-THF: 5,10-methylenetetrahydrofolate.

the reaction is reversible. Adenosine kinase (ADO1) facilitates the consumption of adenosine, further promoting the reversible reaction towards L-homocysteine production.[44] Homocysteine *S*-methyltransferase (MET6) catalyzes the transfer of a methyl group from 5-methyl-tetrahydrofolic acid (5-$CH_3$-THF) to L-homocysteine, regenerating the precursor of SAM, L-methionine. A chimeric yeast-plant methylenetetrahydrofolate reductase (MTHFR) including MTHFR from *S. cerevisiae* (MET13) and MTHFR from *A. thaliana* has been reported to boost the supply of the methyl donor 5-$CH_3$-THF without any feedback inhibition (Fig. 1a).[45] The enhanced *S*-adenosyl-L-methionine pathway, including the above enzyme-coding genes, was finally integrated into the chromosomal locus *YNRCdelta9* of YTP004 to expedite the conversion of eriodictyol to homoeriodicityol.[26] Interestingly, the resulting strain YTP008 achieved a remarkable homoeriodictyol titer of 174.0 mg $L^{-1}$, demonstrating that the reconstruction of both endogenous and heterologous pathways effectively enabled the *de novo* biosynthesis of homoeriodictyol (Fig. 1d).

The results highlighted that the *de novo* synthesis pathway of homoeriodictyol has been successfully constructed in *S. cerevisiae*. The versatile engineering strategies, including the expression of plant-derived enzymes and the modulation of the shikimate pathway, have successfully redirected the carbon flux distribution toward eriodictyol supply, promoting the homoeriodictyol biosynthesis from glucose. The engineered *S. cerevisiae* could serve as a host strain for constructing a cell factory to produce target natural products.

### 3.2. Exploring the missing glycosyltransferases in the homoeriodictyol 7-*O*-glucoside biosynthesis pathway

Homoeriodictyol 7-*O*-glucoside exhibits enhanced bioactivity, improved bioavailability, and reduced cell toxicity compared to its flavonoid aglycone. The glycosyltransferases could achieve the precise glycosylation of homoeriodictyol through a one-step catalyzed reaction in the microbial cell factory, which is more efficient and greener than the multi-step organic reagent-catalyzed reactions in chemical synthesis.[11] The successful biosynthesis of homoeriodictyol 7-*O*-glucoside depends on both the functional glycosyltransferases specific to homoeriodictyol and the effective expression of glycosyltransferases within the chassis strain. To address these concerns, the coding genes of flavonoid 7-*O*-glycosyltransferase from various sources were codon-optimized for functional expression in *S. cerevisiae*, and the performance of each candidate was individually evaluated in strain YTP008 (Fig. 2a).

Flavonoid glycosides are prevalent in plants, indicating that natural sources could be promising for identifying productive glycosyltransferases. To explore this potential, glycosyltransferases known to catalyze the 7-OH position of flavonoids from various plant sources were chosen as the candidates. These glycosyltransferases included *Dic*GT4 from *Dianthus caryophyllus*, and *At*GT2, UGT73C6, and UGT73B2 from *A. thaliana*, as well as *Nt*GT2 from Tobacco. The coding genes of these potential glycosyltransferases were codon-optimized and then inserted into expression frames under the control of the strong constitutive promoter $P_{TEF1}$ and the terminator $T_{ADH1}$. The resulting plasmids carrying the expression cassettes of different glycosyltransferases were transformed into strain YTP008.

Remarkably, these selected glycosyltransferases successfully enabled the synthesis of homoeriodictyol 7-*O*-glucoside, which was detected in 48 h cultures of all the recombinant strains (Fig. 2b and c). The introduction of *Dic*GT4, *At*GT2, *Nt*GT2, UGT73C6, and UGT73B2 yielded homoeriodictyol 7-*O*-glucoside titers of 19.7 mg $L^{-1}$, 68.4 mg $L^{-1}$, 80.7 mg $L^{-1}$, 82.4 mg $L^{-1}$, and 98.2 mg $L^{-1}$, respectively. UGT73C6 and UGT73B2 exhibited superior catalytic abilities, with higher homoeriodictyol 7-*O*-glucoside titers and molar conversion rates compared to other enzymes (Fig. 2c). However, UGT73B2 also exhibited glycosylation activity on other hydroxyl groups of flavanones.[46] Considering the specificity of glycosyltransferase, UGT73C6 was chosen for further studies focused on the 7-OH glycosylation of homoeriodictyol.

These candidate enzymes exhibited similar catalytic abilities in the biosynthesis of flavonoids. *Dic*GT4 is capable of catalyzing the conversion of naringenin into naringenin 7-*O*-glucoside and naringenin 4-*O*-glucoside in *S. cerevisiae*.[47] *At*GT2, UGT73C6, and UGT73B2 all exhibit a preference toward flavanones, with eriodictyol being the most effective substrate for *At*GT2.[48] Both UGT73C6 and UGT73B2 display glycosyltransferase activity toward the 7-OH of naringenin, both *in vivo* and *in vitro*.[46,49] *Nt*GT2, expressed in *E. coli*, successfully converted naringenin into naringenin 7-*O*-glucoside.[50] However, the catalytic efficiency of these enzymes for more complex structures like homoeriodictyol had not been previously characterized. Therefore, the present results demonstrated that the five glycosyltransferases from different plants can be effectively expressed in *S. cerevisiae*, and they are capable of catalyzing the 7-*O*-glycosylation of homoeriodictyol.

Overall, the *de novo* biosynthesis pathway of homoeriodictyol 7-*O*-glucoside was successfully established in *S. cerevisiae*. Identifying effective glycosyltransferases and ensuring their proper expression in a heterologous host facilitated the conversion of homoeriodictyol to its 7-*O*-glucoside form. The results highlighted that certain flavanone and even flavonol 7-*O*-glycosyltransferases are capable of catalyzing the 7-*O*-glycosylation of homoeriodictyol. The newly identified glycosyltransferases demonstrated impressive catalytic efficiency, even without optimization, thereby significantly facilitating the production of homoeriodictyol 7-*O*-glucoside.

### 3.3. Promoting the accumulation of homoeriodictyol 7-*O*-glucoside in *S. cerevisiae*

Homoeriodictyol can be functionalized into homoeriodictyol 7-*O*-glucoside with the assistance of UGT73C6. However, the accumulation of flavonoid *O*-glucosides was hindered by the inherent glycoside hydrolase of *S. cerevisiae*.[47,51] Notably, less homoeriodictyol 7-*O*-glucoside was detected in the 72 h culture compared to the 48 h culture of strain YTP008 expressing UGT73C6 (Fig. S1†). To assess glucoside hydrolysis in the unmodified background, 100 mg $L^{-1}$ of homoeriodictyol 7-*O*-

 

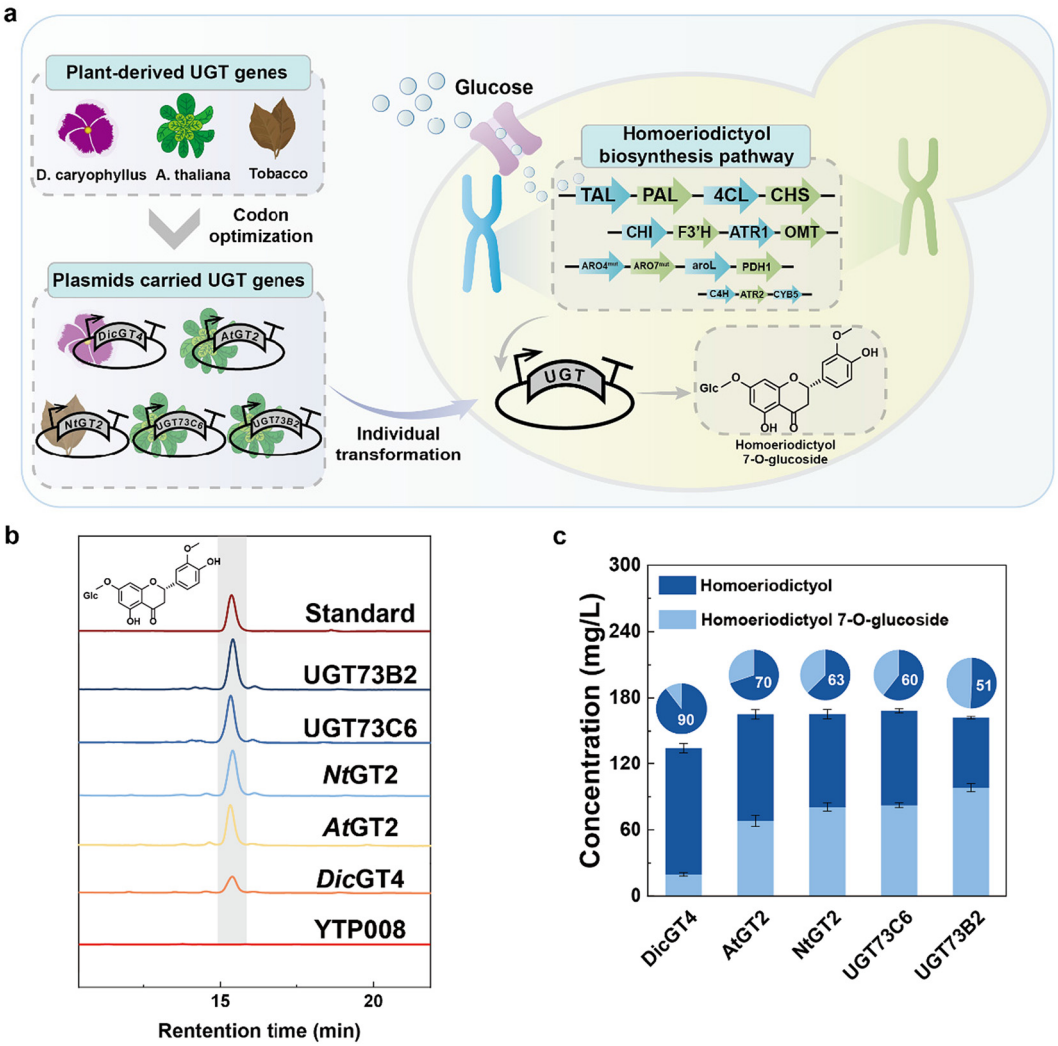


**Fig. 2** The exploration of functional glycosyltransferases for the conversion of homoeriodictyol into homoeriodictyol 7-*O*-glucoside. (a) Schematic illustration of glycosyltransferase screening and identification. (b) The high-performance liquid chromatograms of 48 h fermentation cultures of strains expressing different glycosyltransferases. (c) The production of homoeriodictyol 7-*O*-glucoside and homoeriodictyol in 48 h fermentation cultures of strains expressing different glycosyltransferases. The molar ratios of homoeriodictyol and homoeriodictyol 7-*O*-glucoside under expressing different glycosyltransferases are showcased as pie charts above the bars.

glucoside was added into the cell culture of *S. cerevisiae* strain CEN.PK 2-1D at the onset of fermentation (Fig. 3a). Notably, after 72 h culture, only 73.1 mg $L^{-1}$ of homoeriodictyol 7-*O*-glucoside remained, while 23.9 mg $L^{-1}$ of homoeriodictyol had formed. These results indicated that some homoeriodictyol 7-*O*-glucoside was hydrolyzed into homoeriodictyol. Hence, alleviating the bottlenecks of inherent glycoside hydrolysis in *S. cerevisiae* is crucial for achieving efficient production of homoeriodictyol 7-*O*-glucoside.

Endogenous glucosidases in fungi can cleave the bonds between flavonoid aglycone and glucose groups.[51] In *S. cerevisiae*, the primary glucosidases include GTB1, EGH1, SPR1 and EXG1.[46] To evaluate their roles in hydrolysis, the genes encoding these enzymes were knocked out in strain CEN.PK2-1D. The evaluation of hydrolysis experiment showcased that the deletion of *EXG1* completely eliminated the hydrolysis of homoeriodictyol 7-*O*-glucoside without affecting the cell growth (Fig. 3a). However, knockout of *GTB1*, *EGH1*, and *SPR1* did not significantly impact the hydrolysis of homoeriodictyol 7-*O*-glucoside. The results suggested that these genes had minimal influence on the hydrolysis abilities of endogenous glucosidases.

The effects of knocking out glucosidase-coding genes were further evaluated in a homoeriodictyol 7-*O*-glucoside producing strain. Strain YHG001 was created by integrating the *UGT73C6* expression cassette into the chromosomal locus *YERCdelta8* of strain YTP008. *GTB1*, *EGH1*, *SPR1*, and *EXG1* were individually deleted in YHG001 to generate strains YHG002, YHG003, YHG004, and YHG005, respectively. After 96 h fermentation, strains YHG001, YHG002, YHG003, YHG004, and YHG005 achieved a homoeriodictyol 7-*O*-glucoside tier of 28.2 mg $L^{-1}$, 14.0 mg $L^{-1}$, 24.3 mg $L^{-1}$, 28.4 mg $L^{-1}$,

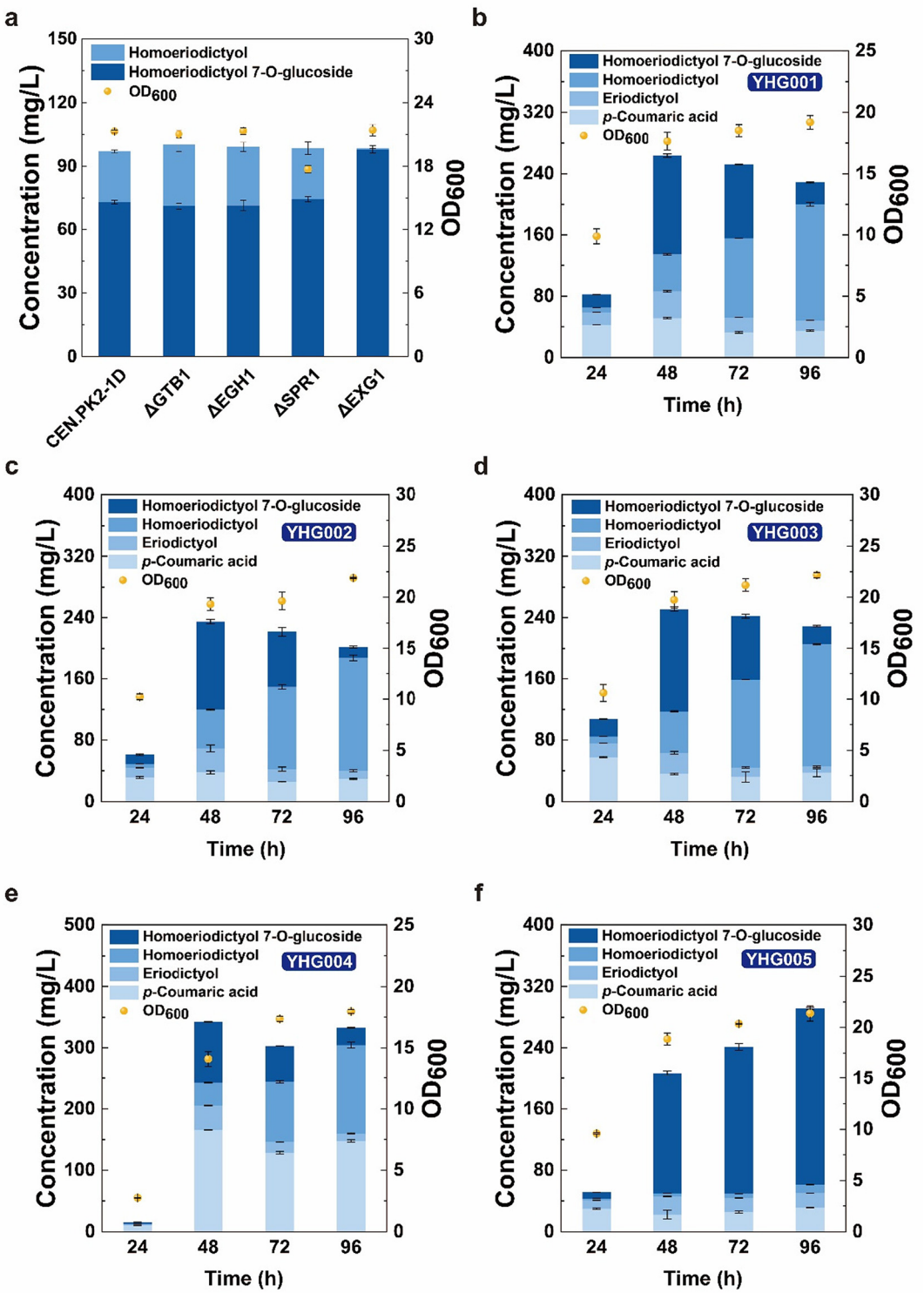


**Fig. 3** Relieving the glycoside hydrolysis to promote the accumulation of homoeriodictyol 7-*O*-glucoside in *S. cerevisiae*. (a) The evaluation of homoeriodictyol 7-*O*-glucoside hydrolysis by *S. cerevisiae* CEN.PK2-1D after the knock-out of glucosidase-coding genes. (b) Profiling 96 h fermentation of strain YHG001. (c–f) The evaluation of homoeriodictyol 7-*O*-glucoside production after the knock-out of GTB1, EGH1, SPR1, and EXG1 in strain YHG001, respectively.

and 230.3 mg $L^{-1}$, respectively. Notably, strain YHG005 achieved a remarkable 7.2-fold increase in the homoeriodictyol 7-*O*-glucoside titer compared to YHG001 (Fig. 3b–f).

In addition to the lower product titers observed in strains YHG001, YHG002, YHG003, and YHG004, a decline in homoeriodictyol 7-*O*-glucoside accumulation was noted after 48 h

 

fermentation (Fig. 3a–e). The deletion of *SPR1* in strain YHG004 resulted in reduced cell density and poor production capacity, with significant accumulation of *p*-coumaric acid throughout the fermentation (Fig. 3e). Previous studies have reported that *SPR1* deletion impaired sporulation due to its role in spore wall assembly.[52] Additionally, the knockout of *EXG1* effectively alleviated the hydrolysis of flavonoid glycoside, consistent with previous findings.[53] This indicated that the deletion of *EXG1* was crucial for enhancing both product accumulation and diverting more carbon fluxes toward homoeriodictyol 7-*O*-glucoside synthesis, thereby confirming EXG1's essential role in flavonoid glycoside hydrolysis.

Overall, the engineering strategy involving the deletion of the glucosidase-coding gene *EXG1* effectively blocked the hydrolysis pathway of homoeriodictyol 7-*O*-glucoside in *S. cerevisiae*. This intervention successfully redirected carbon fluxes towards the synthesis of the target product, achieving a remarkable titer of homoeriodictyol 7-*O*-glucoside. This advancement not only enhances the yield of homoeriodictyol 7-*O*-glucoside but also provides valuable insights for developing yeast cell factories for producing glucosides of other natural products.

### 3.4. Regulating the NADPH supply for homoeriodictyol 7-*O*-glucoside synthesis

The *de novo* biosynthesis pathways of natural products are generally intricate, involving multiple biocatalytic reactions and substantial redox power. The constructed *S. cerevisiae* cell factory yielded a homoeriodictyol 7-*O*-glucoside titer of 191.9 mg $L^{-1}$. However, some intermediates, *p*-coumaric acid and eriodictyol, were remained at the end of the 72 h fermentation. Overexpressing 4CL and ROMT-9$^{mut}$ in strain YHG006 successfully alleviated the accumulation of both two intermediates, resulting in an increased titer of 214.5 mg $L^{-1}$ for homoeriodictyol 7-*O*-glucoside and reflecting an 11.8% improvement compared to strain YHG005 (Fig. 4a). However, approximately 49.2 mg $L^{-1}$ of naringenin was newly observed in the culture of strain YHG006. The overexpression of F3′H and ATR1 did not further channel naringenin into downstream products, possibly due to the inadequate NADPH supply. Multiple reactions in the *de novo* biosynthesis pathway of homoeriodictyol 7-*O*-glucoside, including the P450-mediated conversion of naringenin to eriodictyol, compete for NADPH (Fig. 4b). NADPH is crucial for F3′H to incorporate an oxygen atom into naringenin and acts as an electron donor in the hydroxylation process.[54] Therefore, modulating the intracellular NADPH generation network could considerably relieve naringenin accumulation and improve the efficiency of homoeriodictyol 7-*O*-glucoside production.

Numerous intrinsic metabolic pathways of *S. cerevisiae* are involved in the generation of NADPH. Phosphoglucose dehydrogenase (ZWF1) and 6-phosphoglucose dehydrogenase (GND1) in the pentose phosphate pathway catalyze the reactions requiring the participation of $NADP^+$, contributing to the regeneration of NADPH.[55] Aldehyde dehydrogenase (ALD6) from the pyruvate metabolic pathway is also an $NADP^+$-preferred enzyme, catalyzing the conversion of acetaldehyde to acetate, thereby participating in the regeneration of NADPH. The variant NAD(H)-dependent 2,3-butanediol dehydrogenase (BDH1$^{E221S/I222R/A223S}$) exhibits NADP(H)-dependent properties, potentially increasing the NADPH supply for the homoeriodictyol 7-*O*-glucoside synthesis.[56] Prephenate dehydrogenase (TYR1) in the shikimate pathway converts prephenate into tyrosine while generating NADPH. Additionally, the NADH kinase variant (Pos5Δ17) lacking the mitochondrial targeting sequence can enhance the NADPH pool in the cytoplasm of *S. cerevisiae*.[57] To identify the effectiveness of these genes in NADPH regeneration, ZWF1, TYR1, BDH1$^{E221S/I222R/A223S}$, ALD6, Pos5Δ17, and GND1 were overexpressed under the control of the strong promoter $P_{TEF1}$ in strain YHG006, creating strains YHG007–YHG012, respectively. These engineered strains were then evaluated based on the titers of homoeriodictyol 7-*O*-glucoside and the accumulation of intermediates.

The results demonstrated that overexpressing these genes effectively reduced naringenin accumulation and increased homoeriodictyol 7-*O*-glucoside titers. Notably, the overexpression of Pos5Δ17 and GND1 led to significant increases in homoeriodictyol 7-*O*-glucoside titers, reaching 245.3 mg $L^{-1}$ and 233.5 mg $L^{-1}$, respectively (Fig. 4c). As illustrated in Fig. 4c, integrating the expression cassettes of *Pos5Δ17* and *GND1* into the chromosomal locus *YMRWdelta15* of strain YHG006 resulted in a homoeriodictyol 7-*O*-glucoside titer of 253.6 mg $L^{-1}$, along with a 91.3% reduction in naringenin accumulation for the engineered strain YHG013. It is reported that engineering the NADPH regeneration by overexpressing ZWF1 and GND1 in *Yarrowia lipolytica* also enhanced the conversion of naringenin to eriodictyol.[58] Similarly, overexpressing ZWF1 and ALD6 had been shown to increase the ratio of $NADPH/NADP^+$ in *S. cerevisiae*,[59] potentially alleviating the naringenin accumulation in the present study. Overexpressing TYR1 and BDH1$^{E221S/I222R/A223S}$ benefited the regeneration of NADPH and the function of F3′H in a *S. cerevisiae* cell factory producing taxifolin.[60] The increases in homoeriodictyol 7-*O*-glucoside titers due to the overexpression of ZWF1 and ALD6 were moderate in this study. This could be attributed to the carbon flux being preferentially directed toward the branch pathways, rather than the synthesis pathways of PEP and E4P. The limited availability of PEP and E4P constrained the biosynthesis of downstream aromatic compounds, resulting in only moderate increases in homoeriodictyol 7-*O*-glucoside titers.[39,61] In the present study, overexpressing Pos5Δ17 achieved the most significant improvement in homoeriodictyol 7-*O*-glucoside titer among the single-gene regulations tested, demonstrating its impressive role in NADPH regeneration. All these results showcased that regulating NADPH regeneration can benefit the P450-mediated biocatalytic conversion of naringenin to eriodictyol, ultimately boosting the homoeriodictyol 7-*O*-glucoside production.

The rational regulation strategies for NADPH regeneration effectively alleviated the accumulation of naringenin and improved the homoeriodictyol 7-*O*-glucoside titers, highlighting the critical role of NADPH in the biosynthesis of natural

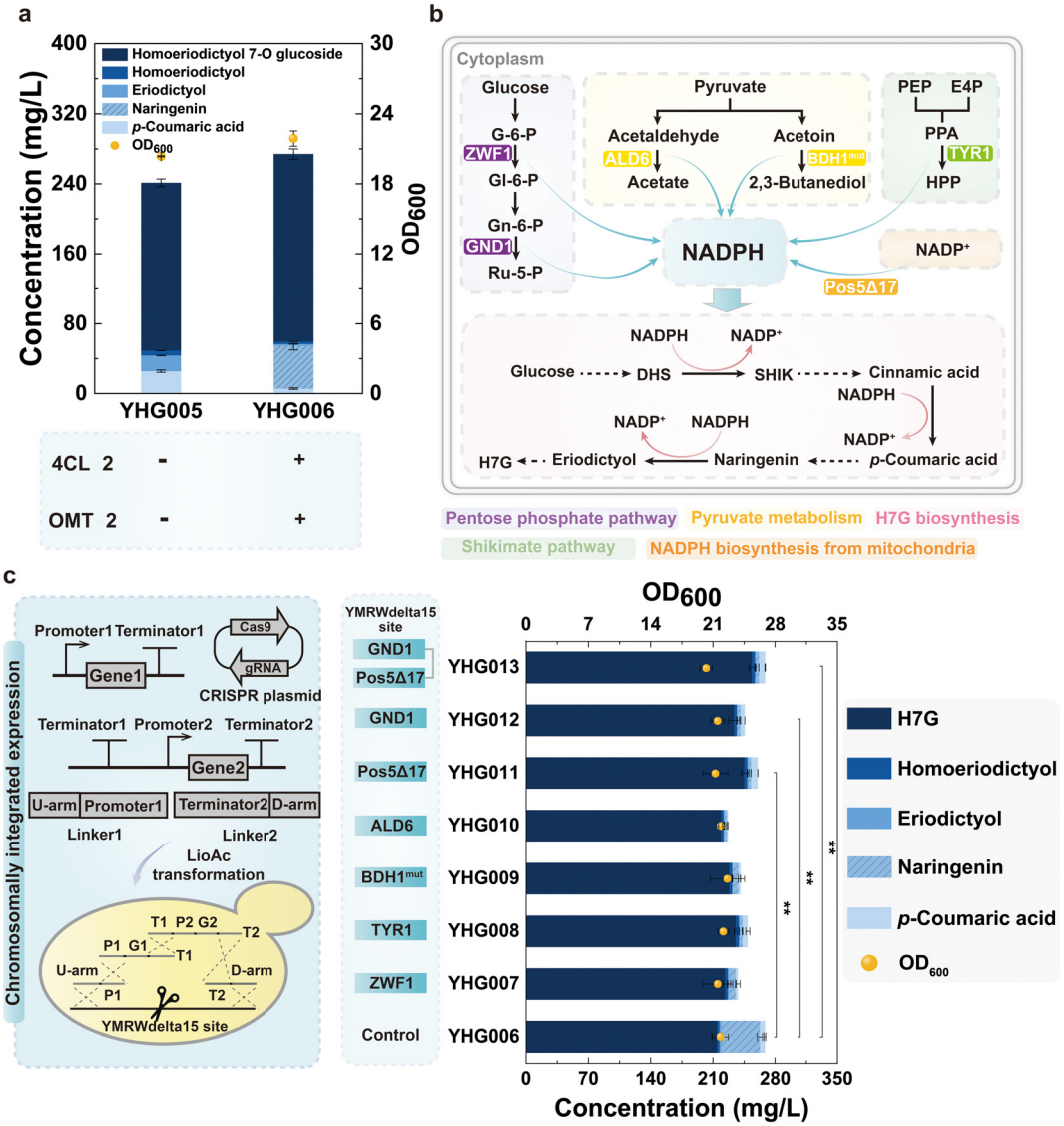


**Fig. 4** Engineering NADPH regeneration to alleviate intermediate accumulation and improve the homoeriodictyol 7-*O*-glucoside titer. (a) Overexpressing key enzymes relieved the intermediate accumulation. (b) Schematic illustration of the NADPH regeneration modules. (c) The biosynthesis performance after augmenting the NADPH supply. *ZWF1*: phosphoglucose dehydrogenase; *GND1*: 6-phosphoglucose dehydrogenase; *ALD6*: aldehyde dehydrogenase; *BDH1*$^{mut}$: the variant of NAD(H)-dependent 2,3-butanediol dehydrogenase; *TYR1*: prephenate dehydrogenase; *Pos5Δ17*: the variant of NADH kinase.

products. All the genes regulated for NADPH regeneration demonstrated positive effects, although some improvements were modest. Therefore, the validated genes show potential as the candidates for enhancing NADPH supply in the microorganisms for other applications. The improvement in microbial synthesis significantly depends on metabolic regulation, highlighting its environmental friendliness and sustainability.

### 3.5. Engineering UDP-glucose supply for homoeriodictyol 7-*O*-glucoside synthesis

Glucose plays a dual role as both a direct precursor for cell growth and the biosynthesis of homoeriodictyol 7-*O*-glucoside. The 7-*O*-glycosylation of homoeriodictyol depends on uridine-5-diphosphate (UDP)-glucose, which provides the glucose group, and UDP-glucose is itself derived from glucose. To boost the homoeriodictyol 7-*O*-glucoside production, the initial glucose concentration in the YPD medium was improved to 30 g $L^{-1}$. As a result, strain YHG013 produced a higher titer of homoeriodictyol 7-*O*-glucoside at 319.0 mg $L^{-1}$ in the medium of 30 g $L^{-1}$ glucose, compared to 20 g $L^{-1}$ glucose medium (Fig. 5a). The homoeriodictyol 7-*O*-glucoside yield showed a decrease from 30 g $L^{-1}$ glucose substrate, which was 10.6 mg $g^{-1}$ glucose. Consequently, efforts were made to enhance the UDP-glucose supply to improve the biosynthesis efficiency of homoeriodictyol 7-*O*-glucoside (Fig. 5b).

UDP-glucose is synthesized from glucose 1-phosphate (G1P), which is derived from the nucleotide sugar biosynthesis pathway, and uridine triphosphate (UTP) from the pyrimidine

 

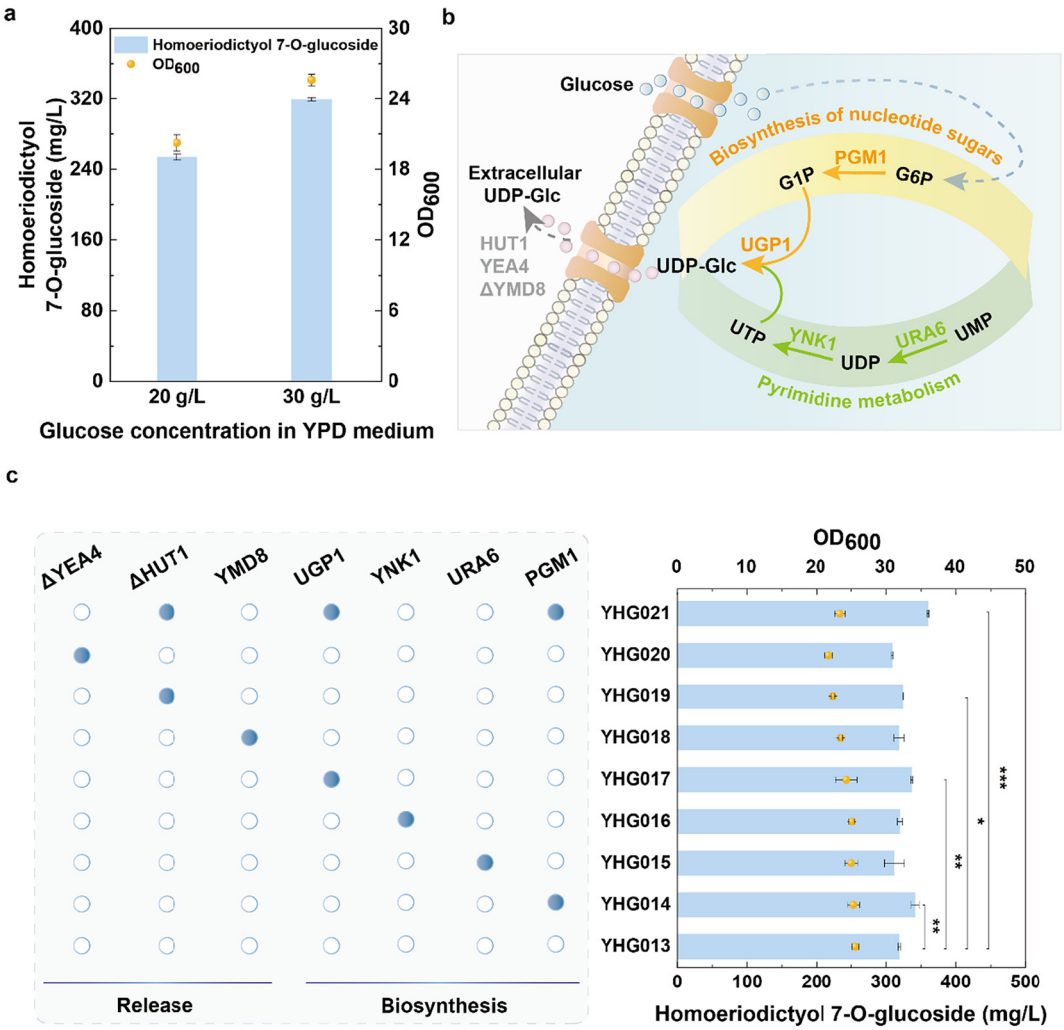


**Fig. 5** Engineering the UDP-glucose supply to boost homoeriodictyol 7-*O*-glucoside production. (a) Schematic illustration of uridine-5-diphosphate-glucose biosynthesis and cellular release. (b) Increased glucose concentration improved the homoeriodictyol 7-*O*-glucoside titer and decreased the homoeriodictyol 7-*O*-glucoside yield. (c) The homoeriodictyol 7-*O*-glucoside production after enhancing the UDP-glucose supply.

metabolism pathway (Fig. 5b). Phosphoglucomutase (PGM1), a key enzyme in the nucleotide sugar biosynthesis pathway, is generally overexpressed to enhance the UDP-glucose supply, since it catalyzes the conversion of glucose-6-phosphate to G1P.[62] Uridylate kinase (URA6) and nucleoside diphosphate kinase (YNK1) are the key enzymes in the UTP biosynthesis pathway. Furthermore, UDP-glucose pyrophosphorylase (UGP1) is responsible for catalyzing the formation of UDP-glucose from G1P and UTP.[63] To strengthen the biosynthesis of UDP-glucose, PGM1, URA6, YNK1, and UGP1 were overexpressed individually in strain YHG013 (Fig. 5c). Strain YHG014 overexpressing PGM1 and strain YHG017 overexpressing UGP1 achieved the homoeriodictyol 7-*O*-glucoside titers of 341.8 mg $L^{-1}$ and 336.9 mg $L^{-1}$, respectively. The overexpression of PGM1 and UGP1 had also been reported to stimulate the UDP-glucose supply and led to an effective increase in the titer of naringenin 7-*O*-glucoside in *S. cerevisiae*.[46] Interestingly, other strains exhibited little improvement in homoeriodictyol 7-*O*-glucoside titers. The results demonstrated that the nucleotide sugar biosynthesis was the limiting factor, while the supply of UTP remained sufficient for the UDP-glucose biosynthesis.

The cellular release of UDP-glucose in *S. cerevisiae* reduces its intracellular concentration, thereby hampering the glycosylation of homoeriodictyol. It has been reported that the knockout of the putative Golgi nucleotide sugar transporter (YMD8) increased the rate of UDP-glucose release. Conversely, deleting UDP-*N*-acetylglucosamine (YEA4) or UDP-galactose transporter (HUT1) led to a reduced rate of UDP-glucose release (Fig. 5b). To inhibit UDP-glucose release, YMD8 was overexpressed, whereas HUT1 and YEA4 were knocked out in strain YHG013 (Fig. 5c). As a result, strain YHG019, lacking HUT1, produced a moderately increased homoeriodictyol 7-*O*-glucoside titer of 324.5 mg $L^{-1}$, while the titer remained unchanged in strain YHG018. However, the deletion of *YEA4* impaired cell growth and decreased homoeriodictyol 7-*O*-glucoside production in

strain YHG020. YEA4 is involved in chitin biosynthesis, an essential component of the fungal cell wall.[64] The lack of YEA4 in strain YHG020 disturbed the formation of the cell wall, which may inhibit cell growth and reduce the productivity.

To further enhance the homoeriodictyol 7-*O*-glucoside production, genome-integrated strategies were employed by inserting the expression cassettes of *PGM1* and *UGP1* into the chromosomal site *YARCdelta8* of strain YHG019. The resulting strain YHG021 achieved a homoeriodictyol 7-*O*-glucoside titer of 360.3 mg $L^{-1}$, representing a 12.9% increase compared to that of strain YHG013. The homoeriodictyol 7-*O*-glucoside yield of strain YHG021 was 12.0 mg $g^{-1}$ glucose, which was 13.3% higher than that of strain YHG013. Enhancing UDP-glucose supply is a proven strategy for microbial synthesis of glycoside. The results highlighted the importance of engineering both UDP-glucose generation and its cellular release for achieving effective glycoside biosynthesis.

Therefore, engineering the UDP-glucose supply effectively redirected carbon fluxes toward the biosynthesis of homoeriodictyol 7-*O*-glucoside. The results suggested that enhancing UDP-glucose biosynthesis is a proven approach to augment the availability of glycosyl donors for homoeriodictyol glycosylation. Besides enhancing UDP-glucose supply, inhibiting its cellular release also holds the promise to encourage the biosynthesis of homoeriodictyol 7-*O*-glucoside. The systematic coordination of engineering both UDP-glucose biosynthesis and cellular release significantly advances the microbial synthesis of glycosides in a *S. cerevisiae* cell factory.

### 3.6. Robustness and fermentation strategies facilitated homoeriodictyol 7-*O*-glucoside production

The constructed *S. cerevisiae* cell factory demonstrated superior synthesis capacity for homoeriodictyol 7-*O*-glucoside. The fermentation profiling of the engineered strains revealed that the trend in homoeriodictyol 7-*O*-glucoside production closely followed the increase in cell biomass (Fig. 3f). Therefore, strategies were developed to extend the cell growth phase of the engineered strain. Additionally, given that glucose serves both as a carbon source and as a direct precursor for homoeriodictyol 7-*O*-glucoside synthesis, the fermentation was optimized by adjusting glucose feeding.

Modulating endogenous growth-related genes could promote the glycosylation process in *S. cerevisiae*.[65] Silent information regulator 2 (SIR2) is involved in extending the lifespan and longevity of *S. cerevisiae* by reducing the accumulation of damaged proteins and DNA through histone deacetylation.[66] Stress-responsive transcriptional activators MSN2 and MSN4, along with the protein kinase RIM15, promote the *S. cerevisiae* growth during starvation by switching the metabolic state to a more robust mode.[67,68] Additionally, oxygen plays a crucial role in both the growth and biosynthesis of aerobic strains. The heterologous expression of VHb from *Vitreoscilla stercoraria* in various host strains was investigated to enhance the cell growth by facilitating the intracellular oxygen uptake.

Overexpression of SIR2, MSN2, MSN4, RIM15, and VHb was conducted in strain YHG021, respectively (Fig. 6a and b). After 72 h fermentation, strain YHG026, overexpressing VHb, achieved an $OD_{600}$ of 24.4 and a homoeriodictyol 7-*O*-glucoside titer of 394.0 mg $L^{-1}$ from 30 g $L^{-1}$ glucose substrate, representing significant increases in both cell biomass and homoeriodictyol 7-*O*-glucoside titer. However, cell biomass and homoeriodictyol 7-*O*-glucoside titers in the remaining strains showed only moderate changes, indicating that starvation stress and DNA damage during the mid to late fermentation stages were not critical factors affecting the performance of the engineered strain. The introduction of VHb also promoted the growth and scutellarin production of the *Y. lipolytica* cell factory, further confirming VHb's role in boosting the oxygen supply in aerobic strains.[69] These results suggested that enhancing intracellular oxygen availability throughout the entire process could facilitate cell growth and catalysis reactions requiring molecule oxygen, thereby increasing the production capacity of engineered strains. The potent regulation strategies for enhancing oxygen supply provided valuable insights for constructing aerobic cell factories.

The fermentation modes were subsequently explored to further improve the homoeriodictyol 7-*O*-glucoside production performance of strain YHG026. In batch fermentation, the homoeriodictyol 7-*O*-glucoside titer increased in a glucose-dependent manner when the glucose concentration increased from 20 g $L^{-1}$ to 30 g $L^{-1}$, reaching 385.0 mg $L^{-1}$ and 434.2 mg $L^{-1}$ at the end of 96 h fermentation, respectively. Further increases in glucose concentration did not result in a higher homoeriodictyol 7-*O*-glucoside titer (Fig. 7a and Table 1). Meanwhile, $OD_{600}$ continued to increase with higher glucose concentration (Fig. 7b). These results indicated that appropriately increasing the glucose concentration in the fermentation medium resulted in an improved titer.

High-density fermentation was also evaluated due to its advantages of increased productivity and more efficient production. Different inoculation concentrations were investigated with initial $OD_{600}$ values of 20, 30, and 40. As shown in Fig. 7c, after 96 h fermentation, the homoeriodictyol 7-*O*-glucoside titer could reach 486.7 mg $L^{-1}$ when the initial $OD_{600}$ was 20, representing a 12.1% increase compared to batch fermentation with a low initial $OD_{600}$ value. The results indicated that increased inoculation concentrations were beneficial for homoeriodictyol 7-*O*-glucoside production. However, further increases in inoculation concentration did not lead to significant improvements in titers. According to the cell growth results (Fig. 7d), enhancing carbon flux toward homoeriodictyol 7-*O*-glucoside may further promote the biosynthesis performance. Notably, the homoeriodictyol 7-*O*-glucoside titer of high-density fermentation in 24 h was approximately 2.2 times that of batch fermentation. This high productivity demonstrated the potential of the high-density fermentation mode for achieving shorter production periods and potentially reducing future commercial production costs.

Fed-batch fermentation possesses the advantage of sustaining the producing phase for a longer period due to the con-

 

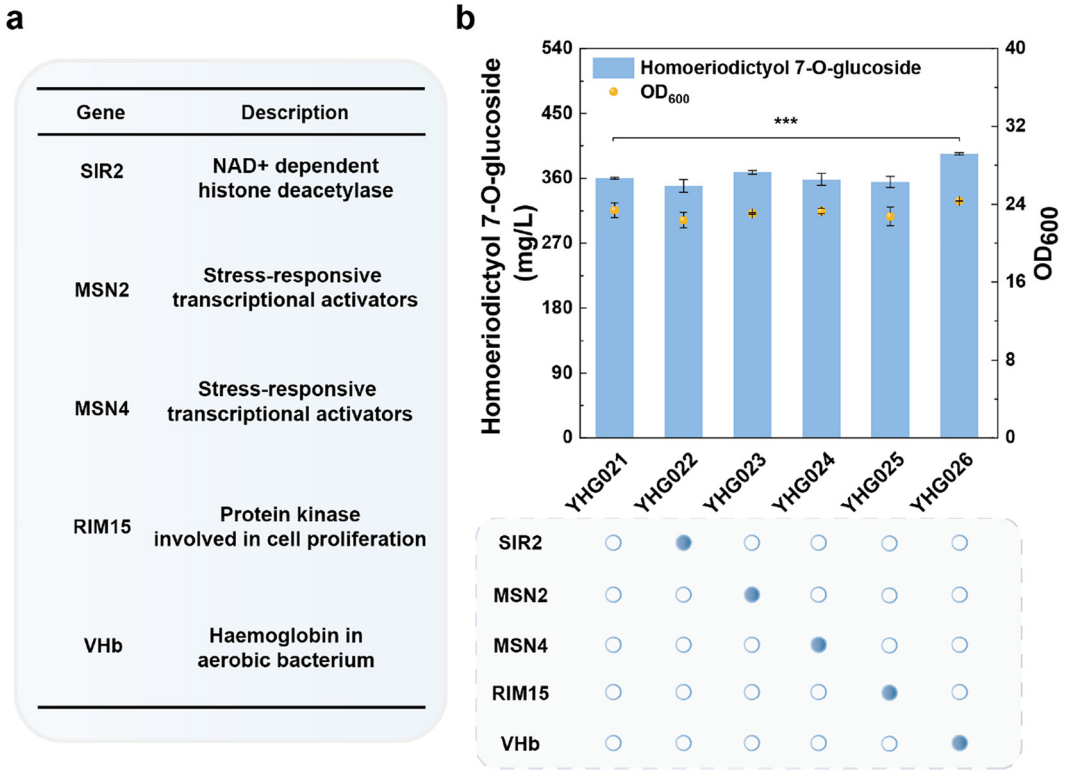


**Fig. 6** Robustness optimization to increase homoeriodictyol 7-*O*-glucoside production. (a) Cell growth regulation details of the engineered strains. (b) Homoeriodictyol production and cell growth after regulating the endogenous related genes.

tinuous supply of nutrients.[70] In this process, 10 g $L^{-1}$ of glucose was added to the fermentation medium at 24 h, or at both 24 h and 48 h, ensuring that the total glucose concentrations in the medium reached 30 g $L^{-1}$ and 40 g $L^{-1}$, respectively. The homoeriodictyol 7-*O*-glucoside titers increased as the glucose concentrations in the medium were elevated from 30 g $L^{-1}$ to 40 g $L^{-1}$, although no significant differences were observed in the $OD_{600}$ trends across different glucose concentrations in the fed-batch fermentation. The phenomenon demonstrated that the fed-batch mode ensured a more equitable contribution of carbon fluxes between cell growth and product biosynthesis. However, the homoeriodictyol 7-*O*-glucoside yields decreased with the increase of glucose concentrations, even with fed-batch fermentation. The homoeriodictyol 7-*O*-glucoside yield was 11.5 mg $g^{-1}$ glucose from 40 g $L^{-1}$ glucose at 96 h of the fed-batch fermentation. The homoeriodictyol 7-*O*-glucoside titers reached 437.4 mg $L^{-1}$ and 461.7 mg $L^{-1}$, respectively, from fed-batch fermentation supplemented with 30 g $L^{-1}$ and 40 g $L^{-1}$ glucose (Fig. 7e and f). This optimization successfully increased the homoeriodictyol 7-*O*-glucoside titer by approximately 20.0%, compared to batch fermentation with 20 g $L^{-1}$ glucose. Additionally, *p*-coumaric acid was supplemented as a precursor to boost the homoeriodictyol 7-*O*-glucoside production. The homoeriodictyol 7-*O*-glucoside titer reached 600.2 mg $L^{-1}$ in the fed-batch fermentation with 40 g $L^{-1}$ glucose and 250 mg $L^{-1}$ *p*-coumaric acid. These results indicated that co-feeding *p*-coumaric acid and glucose enabled a more efficient production of homoeriodictyol 7-*O*-glucoside in the *S. cerevisiae* cell factory.

For the green large-scale production of homoeriodictyol 7-*O*-glucoside in the *S. cerevisiae* cell factory, it is important to explore suitable strategies for separating homoeriodictyol 7-*O*-glucoside from the fermentation broth. For example, macroporous resin and membranes have been reported to be capable of purifying flavonoid glycoside at the end of fermentation.[71–73] Typically, the supernatant of the fermentation broth is mixed with macroporous resin. After static or dynamic adsorption, the resin is treated with ethanol–water solution to elute the products. The eluent is then collected and evaporated to dryness.[73] As for membrane separation, the fermentation supernatant containing the natural product is retained by certain membrane pore sizes and pressures. The retained solution is then vacuum-dried.[71] Both separation methods are operated under mild conditions with less solvent requirements. Integrating advanced green separation strategies with the present study would promote the feasibility of homoeriodictyol 7-*O*-glucoside production and contribute to its scale-up with a green production model.[74]

Additionally, the versatile microbial cell factory enabled efficient biosynthesis of a valuable flavonoid, homoeriodictyol 7-*O*-glucoside. The biosynthesis pathway uses inexpensive raw materials and achieves a highest yield of 13.1 mg $g^{-1}$. The novel biosynthesis approach offers a more environmentally friendly alternative, with an *E*-factor of 1667. The utilization of renewable glucose as the substrate makes it a more sustainable

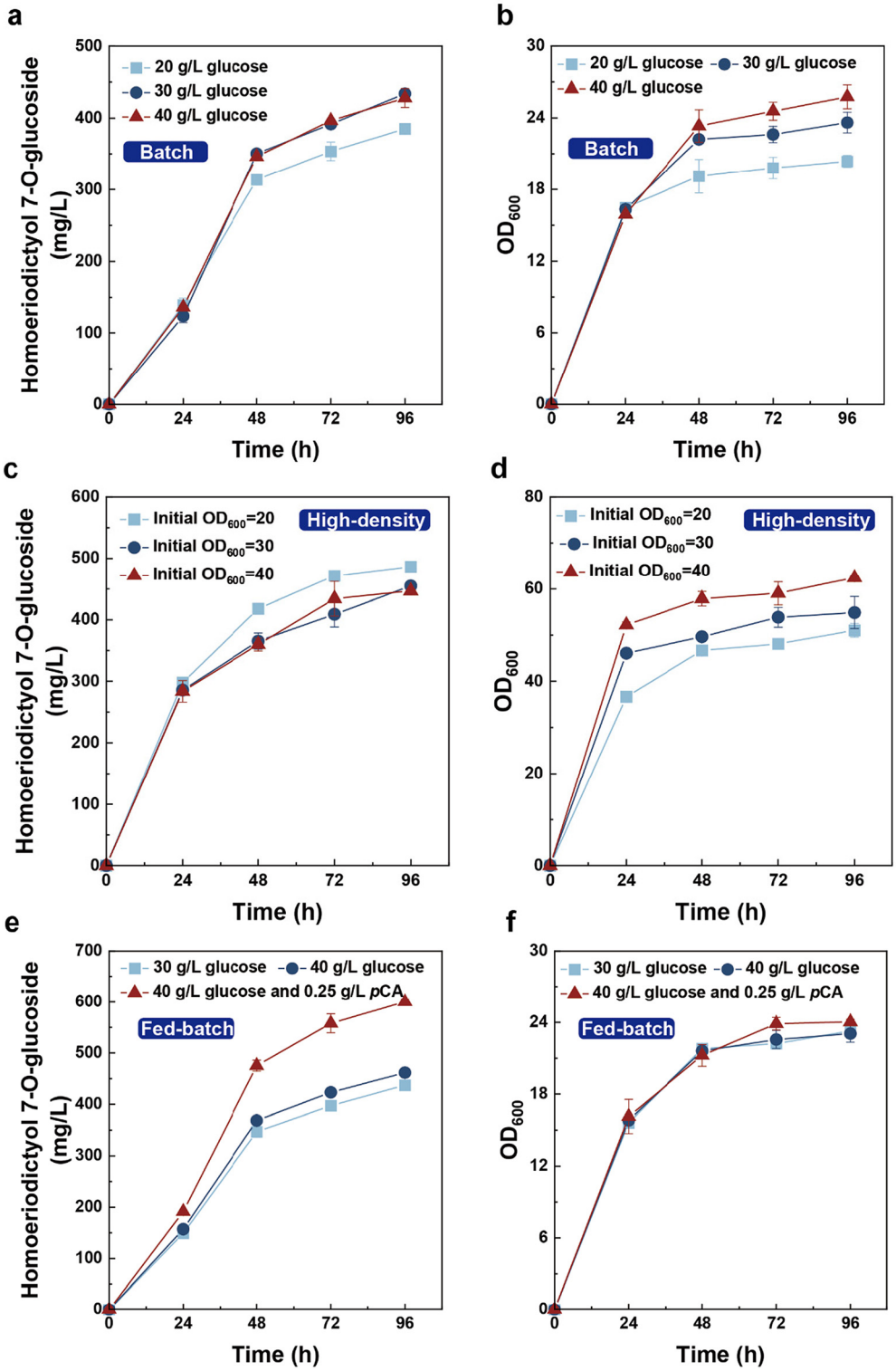


**Fig. 7** Effective production of homoeriodictyol 7-*O*-glucoside through fermentation optimization strategy design. (a and b) The homoeriodictyol 7-*O*-glucoside production and biomass of strain YHG026 through 96 h batch fermentation with various concentrations of glucose. (c and d) The homoeriodictyol 7-*O*-glucoside production and biomass of strain YHG026 through 96 h high-density fermentation with different inoculation concentrations. (e and f) The homoeriodictyol 7-*O*-glucoside production and biomass of strain YHG026 through 96 h fed-batch fermentation with different concentrations of glucose or supplementation with *p*-coumaric acid.

Table 1 Metabolic engineering strategies that promoted the production of homoeriodictyol 7-*O*-glucoside

| Strategies | Glucose concentration (g $L^{-1}$) | Eriodictyol (mg $L^{-1}$) | Homoeriodictyol (mg $L^{-1}$) | Homoeriodictyol 7-*O*-glucoside (mg $L^{-1}$) | Yield (mg $g^{-1}$) | Fermentation modes |
|---|---|---|---|---|---|---|
| Construction of TAL pathway | 20 | 15.2 | n.d. | n.d. | 0.76 | Batch |
| Construction of PAL pathway | 20 | 109.9 | n.d. | n.d. | 5.5 | Batch |
| Enhancing shikimate pathway | 20 | 209.2 | n.d. | n.d. | 10.5 | Batch |
| Modulating methylation pathway | 20 | 6.6 | 174.0 | n.d. | 8.7 | Batch |
| Construction of glycosylation pathway | 20 | 19.5 | 103.2 | 96.6 | 4.8 | Batch |
| Relieving the glycoside hydrolysis | 20 | 18.0 | 5.6 | 191.9 | 9.6 | Batch |
| Overexpressing key enzymes | 20 | 2.0 | 2.7 | 214.5 | 10.7 | Batch |
| Engineering NADPH regeneration | 20 | 0.71 | 3.6 | 253.6 | 12.7 | Batch |
| Engineering UDP-glucose supply | 30 | 0.57 | 4.9 | 360.3 | 12.0 | Batch |
| Robustness optimization | 30 | 1.2 | 2.3 | 394.0 | 13.1 | Batch |
| Batch fermentation | 40 | 2.5 | 2.1 | 428.1 (96 h) | 10.7 | Batch |
| High-density fermentation | 40 | 5.1 | 0.94 | 486.7 (96 h) | 12.2 | High-density |
| Fed-batch fermentation | 40 | 4.4 | 2.6 | 461.7 (96 h) | 11.5 | Fed-batch |

TAL represents the tyrosine branch; PAL represents the phenylalanine branch. All the titers and yields refer to the results of 72 h fermentation, unless otherwise specified. Yields refer to the yields of the final products.



process with higher carbon utilization efficiency (Table S3†). This is the first report of the *de novo* biosynthesis of homoeriodictyol 7-*O*-glucoside, and a record titer of 600.2 mg $L^{-1}$ has been achieved. The novel biosynthetic approach provides a greener and more efficient route for synthesizing valuable natural products like homoeriodictyol 7-*O*-glucoside.

Overall, various engineering strategies for the *S. cerevisiae* cell factory had been designed by optimizing the internal and external environments to encourage the homoeriodictyol 7-*O*-glucoside production. Synergistically strengthening oxygen uptake and increasing glucose concentration significantly benefited both cell growth and homoeriodictyol 7-*O*-glucoside production. The construction and regulation of *de novo* biosynthesis yielded a record titer of homoeriodictyol 7-*O*-glucoside.

## 4. Conclusions

The promising *S. cerevisiae* cell factory was designed and regulated for the *de novo* biosynthesis of homoeriodictyol 7-*O*-glucoside. Key metabolic strategies enabled the effective homoeriodictyol 7-*O*-glucoside synthesis in this versatile microbial cell factory. An efficient biosynthesis pathway of homoeriodictyol was established to funnel tyrosine and phenylalanine into flavonoids through precise tuning of inherent metabolic modules. By mining glycosyltransferases and inhibiting glycoside hydrolysis, homoeriodictyol 7-*O*-glucoside was biosynthesized in *S. cerevisiae* for the first time. Additionally, regulating NADPH regeneration and UDP-glucose supply alleviated the intermediate accumulation and promoted the homoeriodictyol 7-*O*-glucoside production. Together with fermentation optimization, the *S. cerevisiae* cell factory achieved a record homoeriodictyol 7-*O*-glucoside titer of 600.2 mg $L^{-1}$ and the yield of 12.2 mg $g^{-1}$ glucose. Overall, metabolic engineering strategies have enabled the microbial cell factory to efficiently synthesize a flavonoid glycoside, contributing to the green and sustainable biosynthesis of natural products.

## Data availability

The data supporting this article have been included as part of the ESI.†

## Conflicts of interest

The authors declare no competing interests.

## Acknowledgements

This work was supported by the National Key Research and Development Program of China (2023YFC3403500).

## References

1 X. Xu, Y. Liu, G. Du, R. Ledesma-Amaro and L. Liu, *Trends Biotechnol.*, 2020, **38**, 779–796.
2 H.-N. Lan, R.-Y. Liu, Z.-H. Liu, X. Li, B.-Z. Li and Y.-J. Yuan, *Biotechnol. Adv.*, 2023, **64**, 108107.
3 M. C. Dias, D. C. Pinto and A. M. Silva, *Molecules*, 2021, **26**, 5377.
4 A. Roy, A. Khan, I. Ahmad, S. Alghamdi, B. S. Rajab, A. O. Babalghith, M. Y. Alshahrani, S. Islam and M. R. Islam, *Biomed Res. Int.*, 2022, **2022**, 445291.
5 L. R. Beltran, S. Sterneder, A. Hasural, S. Paetz, J. Hans, J. P. Ley and V. Somoza, *Pharmaceuticals*, 2022, **15**, 317.
6 K. I. Liszt, J. Hans, J. P. Ley, E. Kock and V. Somoza, *J. Agric. Food Chem.*, 2018, **66**, 2295–2300.
7 C. M. Hochkogler, K. Liszt, B. Lieder, V. Stoger, A. Stubler, M. Pignitter, J. Hans, S. Widder, J. P. Ley, G. E. Krammer and V. Somoza, *Mol. Nutr. Food Res.*, 2017, **61**, 1700459.
8 S.-Y. Zhu, N. Li, Z.-H. Liu, Y.-J. Yuan and B.-Z. Li, *Green Carbon*, 2025, DOI: 10.1016/j.greenca.2024.11.005.
9 B. Hofer, *Appl. Microbiol. Biotechnol.*, 2016, **100**, 4269–4281.

10 Y. Ji, B. Li, M. Qiao, J. Li, H. Xu, L. Zhang and X. Zhang, *Appl. Microbiol. Biotechnol.*, 2020, **104**, 6587–6600.
11 M. Kang, Z. Ma, B. Liu, D. Pan and J. Li, *Chin. J. Org. Chem.*, 2017, **37**, 1516–1522.
12 J. Huang, Y. J. Lu, C. Guo, S. Zuo, J. L. Zhou, W. L. Wong and B. Huang, *J. Sci. Food Agric.*, 2021, **101**, 5163–5171.
13 K. R. Choi and S. Y. Lee, *Nat. Rev. Bioeng.*, 2023, **1**, 832–857.
14 M. Kourgiantaki, V. P. Demertzidou and A. L. Zografos, *Org. Lett.*, 2022, **24**, 8476–8480.
15 S. E. Reisman and T. J. Maimone, *Acc. Chem. Res.*, 2021, **54**, 1815–1816.
16 T. Fukunaga, I. Kajikawa, K. Nishiya, Y. Watanabe, K. Takeya and H. Itokawa, *Chem. Pharm. Bull.*, 1987, **35**, 3292–3297.
17 J. Yin, N. Han, X. Xu, Z. Liu, B. Zhang and S. Kadota, *Planta Med.*, 2008, **74**, 120–125.
18 A. Cravens, J. Payne and C. D. Smolke, *Nat. Commun.*, 2019, **10**, 2142.
19 D. Yang, S. Y. Park, Y. S. Park, H. Eun and S. Y. Lee, *Trends Biotechnol.*, 2020, **38**, 745–765.
20 H. Liu, X. Tao, S. Ntakirutimana, Z.-H. Liu, B.-Z. Li and Y.-J. Yuan, *Chem. Eng. J.*, 2024, **495**, 153375.
21 H. Cui, M. C. Song, J. Y. Lee and Y. J. Yoon, *J. Ind. Microbiol. Biotechnol.*, 2019, **46**, 1707–1713.
22 R. Ni, M. Niu, J. Fu, H. Tan, T. T. Zhu, J. Zhang, H. X. Lou, P. Zhang, J. X. Li and A. X. Cheng, *J. Integr. Plant Biol.*, 2022, **64**, 1935–1951.
23 M. S. Dunstan, C. J. Robinson, A. J. Jervis, C. Yan, P. Carbonell, K. A. Hollywood, A. Currin, N. Swainston, R. L. Feuvre, J. Micklefield, J.-L. Faulon, R. Breitling, N. Turner, E. Takano and N. S. Scrutton, *Synth. Biol.*, 2020, **5**, ysaa012.
24 B. Peng, L. Zhang, S. He, R. Oerlemans, W. J. Quax, M. R. Groves and K. Haslinger, *J. Agric. Food Chem.*, 2024, **72**, 529–539.
25 Á. Pérez-Valero, J. Serna-Diestro, A. Tafur Rangel, S. Barbuto Ferraiuolo, C. Schiraldi, E. J. Kerkhoven, C. J. Villar and F. Lombó, *Int. J. Mol. Sci.*, 2024, **25**, 4053.
26 S.-Y. Zhu, S.-C. Liu, C.-X. Zhang, X. Xin, Z.-H. Liu, L.-J. Zhang, B.-Z. Li and Y.-J. Yuan, *Green Chem.*, 2024, **26**, 5260–5272.
27 H. Fang, D. Li, J. Kang, P. Jiang, J. Sun and D. Zhang, *Nat. Commun.*, 2018, **9**, 4917.
28 J. Guo, D. Gao, J. Lian and Y. Qu, *Nat. Commun.*, 2024, **15**, 457.
29 P. E. Hodges, A. H. Z. McKee, B. P. Davis, W. E. Payne and J. I. Garrels, *Nucleic Acids Res.*, 1999, **27**, 69–73.
30 R. D. Gietz and R. H. Schiestl, *Nat. Protoc.*, 2007, **2**, 31–34.
31 G. Sezonov, D. Joseleau-Petit and R. D'Ari, *J. Bacteriol.*, 2007, **189**, 8746–8749.
32 T. L. Orr-Weaver, J. W. Szostak and R. J. Rothstein, *Proc. Natl. Acad. Sci. U. S. A.*, 1981, **78**, 6354–6358.
33 M. Jinek, K. Chylinski, I. Fonfara, M. Hauer, E. Charpentier and J. A. Doudna, *Science*, 2012, **337**, 816–821.
34 S. Gao, Y. Lyu, W. Zeng, G. Du, J. Zhou and J. Chen, *J. Agric. Food Chem.*, 2020, **68**, 1015–1021.
35 S. Zhang, J. Liu, Z. Xiao, X. Tan, Y. Wang, Y. Zhao, N. Jiang and Y. Shan, *J. Fungi*, 2024, **10**, 119.
36 J. Mao, M. T. Mohedano, J. Fu, X. Li, Q. Liu, J. Nielsen, V. Siewers and Y. Chen, *Metab. Eng.*, 2023, **79**, 192–202.
37 R. Bisquert, A. Planells-Cárcel, E. Valera-García, J. M. Guillamón and S. Muñiz-Calvo, *Microb. Biotechnol.*, 2022, **15**, 1499–1510.
38 L. Meng, M. Diao, Q. Wang, L. Peng, J. Li and N. Xie, *Microb. Cell Fact.*, 2023, **22**, 46.
39 Q. Liu, T. Yu, X. Li, Y. Chen, K. Campbell, J. Nielsen and Y. Chen, *Nat. Commun.*, 2019, **10**, 4976.
40 M. Tous Mohedano, J. Mao and Y. Chen, *ACS Synth. Biol.*, 2023, **12**, 144–152.
41 Y. Chen, L. Daviet, M. Schalk, V. Siewers and J. Nielsen, *Metab. Eng.*, 2013, **15**, 48–54.
42 S. Shi, Y. Chen, V. Siewers and J. Nielsen, *mBio*, 2014, **5**, e01130–e01114.
43 Q. Liu, L. Liu, J. Zhou, H.-d. Shin, R. R. Chen, C. Madzak, J. Li, G. Du and J. Chen, *J. Biotechnol.*, 2013, **167**, 472–478.
44 R. Chen, J. Gao, W. Yu, X. Chen, X. Zhai, Y. Chen, L. Zhang and Y. J. Zhou, *Nat. Chem. Biol.*, 2022, **18**, 520–529.
45 S. Roje, S. Y. Chan, F. Kaplan, R. K. Raymond, D. W. Horne, D. R. Appling and A. D. Hanson, *J. Biol. Chem.*, 2002, **277**, 4056–4061.
46 H. Li, W. Ma, Y. Lyv, S. Gao and J. Zhou, *ACS Synth. Biol.*, 2022, **11**, 2339–2347.
47 S. R. Werner and J. A. Morgan, *Bioprocess. Biosyst. Eng.*, 2010, **33**, 863–871.
48 J. H. Kim, B. G. Kim, Y. Park, J. H. Ko, C. E. Lim, J. Lim, Y. Lim and J. H. Ahn, *Biosci. Biotechnol. Biochem.*, 2006, **70**, 1471–1477.
49 P. Jones, B. Messner, J. Nakajima, A. R. Schäffner and K. Saito, *J. Biol. Chem.*, 2003, **278**, 43910–43918.
50 N. Dorjjugder and G. Taguchi, *Appl. Biochem. Biotechnol.*, 2022, **194**, 3320–3329.
51 H. McMahon, B. W. Zoecklein, K. Fugelsang and Y. Jasinski, *J. Ind. Microbiol. Biotechnol.*, 1999, **23**, 198–203.
52 G. Lesage and H. Bussey, *Microbiol. Mol. Biol. Rev.*, 2006, **70**, 317–343.
53 S. Schmidt, S. Rainieri, S. Witte, U. Matern and S. Martens, *Appl. Environ. Microbiol.*, 2011, **77**, 1751–1757.
54 R. D. Ceccoli, D. A. Bianchi and D. V. Rial, *Front. Microbiol.*, 2014, **5**, 25.
55 S. W. Gorsich, B. S. Dien, N. N. Nichols, P. J. Slininger, Z. L. Liu and C. D. Skory, *Appl. Microbiol. Biotechnol.*, 2006, **71**, 339–349.
56 M. Ehsani, M. R. Fernández, J. A. Biosca and S. Dequin, *Biotechnol. Bioeng.*, 2009, **104**, 381–389.
57 T. Yukawa, T. Bamba, G. Guirimand, M. Matsuda, T. Hasunuma and A. Kondo, *Biotechnol. Bioeng.*, 2021, **118**, 175–185.
58 M. Yue, M. Liu, S. Gao, X. Ren, S. Zhou, Y. Rao and J. Zhou, *J. Agric. Food Chem.*, 2024, **72**, 4292–4300.
59 X. Wang, Z. Liang, J. Hou, X. Bao and Y. Shen, *BMC Biotechnol.*, 2016, **16**, 31.

 

60 J. Yang, J. Liang, L. Shao, L. Liu, K. Gao, J. L. Zhang, Z. Sun, W. Xu, P. Lin, R. Yu and J. Zi, *Metab. Eng.*, 2020, **59**, 44–52.
61 J.-E. Kim, I.-S. Jang, B. H. Sung, S. C. Kim and J. Y. Lee, *Sci. Rep.*, 2018, **8**, 15820.
62 T. Liu, Y. Liu, L. Li, X. Liu, Z. Guo, J. Cheng, X. Zhu, L. Lu, J. Zhang, G. Fan, N. Xie, J. Lu and H. Jiang, *J. Agric. Food Chem.*, 2021, **69**, 5917–5925.
63 Y. Mao, Z. Chen, Y. Ren, Y. Sun and Y. Wang, *J. Agric. Food Chem.*, 2021, **69**, 13155–13163.
64 M. D. Lenardon, C. A. Munro and N. A. Gow, *Curr. Opin. Microbiol.*, 2010, **13**, 416–423.
65 S. Li, S. Luo, X. Zhao, S. Gao, X. Shan, J. Lu and J. Zhou, *J. Agric. Food Chem.*, 2024, **72**, 8140–8148.
66 W. Grabowska, E. Sikora and A. Bielak-Zmijewska, *Biogerontology*, 2017, **18**, 447–476.
67 Z. Kuang, S. Pinglay, H. Ji and J. D. Boeke, *eLife*, 2017, **6**, e29938.
68 X.-Q. Wang, B. Yuan, F.-L. Zhang, C.-G. Liu, C. Auesukaree and X.-Q. Zhao, *Antioxidants*, 2024, **13**, 260.
69 P. Zhang, W. Wei, Y. Shang and B.-C. Ye, *Bioresour. Technol.*, 2023, **385**, 129421.
70 P. van Hoek, E. de Hulster, J. P. van Dijken and J. T. Pronk, *Biotechnol. Bioeng.*, 2000, **68**, 517–523.
71 T. Chen, H. M. Li, D. L. Zou, Y. Z. Du, Y. H. Shen and Y. Li, *J. Sep. Sci.*, 2014, **37**, 3760–3766.
72 S. Zhao, X. Wu, X. Duan, C. Zhou, Z. Zhao, H. Chen, Z. Tang, Y. Wan, Y. Xiao and H. Chen, *PeerJ*, 2021, **9**, e11223.
73 Y. Wu, H. Wang, Y. Liu, L. Zhao and J. Pei, *Biotechnol. Biofuels*, 2022, **15**, 129.
74 L. Zhang, T. Wu, W. Xiao, Z. Wang, G. Ding and L. Zhao, *Molecules*, 2018, **23**, 1167.